VISUALISATION AND ANALYSIS OF THE FLUID FLOW STRUCTURE INSIDE AN ELLIPTICAL STEELMAKING LADLE THROUGH IMAGE PROCESSING TECHNIQUES

R.P. NUNES[1]*, J.A.M. PEREIRA[2], A.C.F. VILELA[2], F.T.V. DER LAAN[3]

Universidade Federal do Rio Grande do Sul

[1] Departamento de Física Teórica, Instituto de Física,
P. O. Box 15051, 91501-970, Porto Alegre, RS, BRASIL.

[2]Departamento de Metalurgia, Escola de Engenharia
Av. Bento Gonçalves 9500, Setor 6, C. T., Sala 222, 91501-970, Porto Alegre, RS, BRASIL.

[3] Departamento de Engenharia Nuclear, Escola de Engenharia,
Av. Osvaldo Aranha 99, 4o. andar, 90046-900, Porto Alegre, RS, BRASIL.
* Corresponding Author: roger.pizzato@ufrgs.br

Abstract

The understanding of the fluid flow conditions during the liquid steel stirring treatment in the ladle is an important issue to optimize the steelmaking process. In this sense, in this article, a cold physical model in reduced scale of a gas-stirred ladle has been built and investigated through image processing techniques to evaluate its velocity field. The gas has been injected in 3 different positions of the ladle base and the resulted fluid flow has been analyzed by the Image Processing Velocimetry technique, using the PIV mode (Particle Image Velocimetry). Such analysis was qualitative and aimed at verifying and at understanding previously obtained results through dye tracer tests and mixing times. Whenever it has been possible, our results have been compared with other ones found in the literature.

Keywords: physical model, secondary refining, gas-stirred ladle, particle image velocimetry.

Nomenclatures

PT1	Eccentric gas-injection position
PT2	Half radius gas-injection position
PT3	Central gas-injection position
Q_{ladel}	The gas flow rate of the industrial ladle ($m^3.s^{-1}$)
Q_{model}	The gas flow rate of the ladle's model ($m^3.s^{-1}$)

Greek Symbol

λ	The scale factor between the real and the modelled ladle

---

1. Introduction

During the secondary refine step, which is commonly named as metallurgy in ladle, the liquid steel is stirred with inert gas for the final adjustment of its chemical and its thermal composition. The refining reactions of metal/slag are intensified and the inclusions are removed by a thin layer of slag in the bath surface.

In order to optimize different metallurgical stages in gas-stirred ladles, physical models have been used as tools to study chemical and physical phenomena under the influence of operational variables during the liquid steel stirring treatment [1].

Studies on mixing in gas-stirred ladles [2, 3, 4, 5, 6] show that the fluid flow structure inside the ladle is one of the main control parameters of the mixing process. Considering that the apparatus employed in the experiments is unchanged, one way of modifying the fluid flow structure inside the ladle is to stir it with different gas-injection positions. The gas injection position variation determines each type of fluid flow which is obtained and has influence in a higher or lower degree over the mixing characteristics. A given mixing is considered better when the analyzed fluid becomes more homogeneous in a shorter time.

Besides the last purpose, a mixing time reduction in the industry assures the increase of productivity and the reduction of the accessory products employed in the steelmaking process, as an example, the Argon gas. Therefore, as a resume, when the interest falls in the increment of the quality on the overall metallurgical process, complete understanding on fluid flow conditions which take place during the liquid steel stirring in the ladle is essential.

In this sense, this paper aims at analyzing the characteristics of the liquid steel flow obtained from the injection of gas in 3 different positions of the ladle base under the influence of different operational parameters during the mixing stage of the steelmaking process.

For this, a physical model of an industrial ladle with an elliptical shape has been built in acrylic and cross-sectioned by two orthogonal LASER sheets. The gas injection position has been set to three different points of the ladle bottom.

The resultant velocity field in two dimensions have been measured for each one of these 6 configurations by the means of the image processing velocimetry technique, using the PIV mode [7]. The analysis of these measured velocity fields will determine the influence of each gas injection position over the generated fluid flow. The obtained results will be compared with previously information obtained by us through dye tracer tests and mixing time [12].

This article is organised in the following form: in section 2, the methodology employed in the experiments is presented. The developed physical model is described and the experimental techniques used in this works such as the dye tracer test, mixing time, and PIV are briefly exposed. In section 3, the two-dimensional velocity fields measured in the tests for each one of the previously commented gas injection positions and LASER Sheets are shown. In this section, a long discussion about the obtained results is also established. In section 4, the conclusions are presented. Finally, in section 5, the perspectives for future works are discussed.

2. Methodology

2.1 Physical model

Fig. 1 presents, without the correct aspect ratio, the physical model of a gas-stirred ladle with an elliptical transversal section employed in the tests. The ladle semi major axis has 346,5mm and its semi minor axis has 380,3mm. Its height is 820mm. The physical model has been built in acrylic (Plexiglas), with reduced scale of 1:3, and it uses water at room temperature as a steel simulator. The bath is agitated by compressed air injection at the ladle bottom in three different injection positions, such as PT1 (eccentric test position), PT2 (half radius test position) and PT3 (central test position). Those gas injection positions are commonly used here by some local industries.
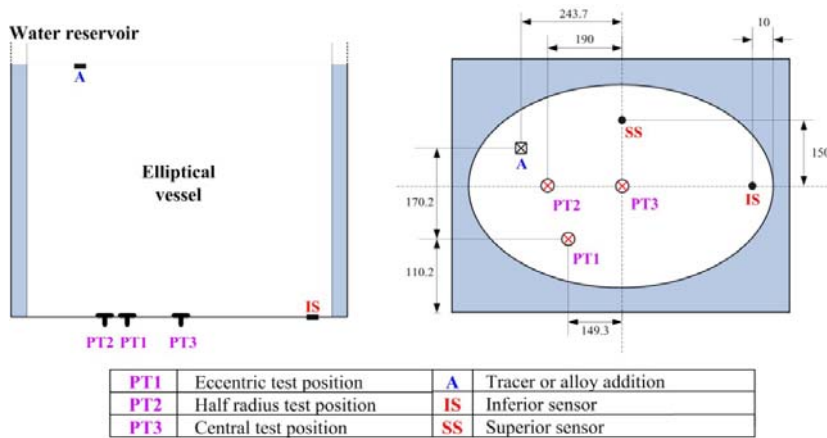

PT1	Eccentric test position	A	Tracer or alloy addition
PT2	Half radius test position	IS	Inferior sensor
PT3	Central test position	SS	Superior sensor

Fig. 1. Frontal and Superior Views of the Ladle's Physical Model Employed in the Tests.

Measures of mixing times have been carried out by the means of two conductivity sensors: SS (Superior Sensor), immersed 90 mm below of the surface of the bath and displaced at 150 mm of the center of the ladle in the direction of the smaller radius, and IS (Inferior Sensor), introduced in the edge of the greater radius of the ladle, at 10mm of its bottom and at 30mm of its wall. The localization of the tracer addition position (A) can also be observed in Fig. 1.

For the minimisation of the effects of optical distortions on the frames captured through the CCD camera employed in the PIV measurements discussed in the subsection 2.4, which are a natural consequence of the elliptical ladle shape, the ladle physical model has been inserted in a transparent and rectangular reservoir filled with water.

Table 1 shows a summary of the most important parameters of the developed physical model and of a typical ladle used here in a local industry. The equivalence between the physical model and the industrial ladle is described by a geometric similarity, through a scale factor (λ), and a dynamic similarity, derived from the equality of the Froude number. By the way, considering these criterions for the calculation of the gas flow rate in the physical model Q_{model}, the equation 1 showed below has been assumed from Mazumder [9, 10]:

$$Q_{model} = \lambda^{5/2} Q_{ladle} \tag{1}$$

in which Q_{ladle} is the gas flow rate (in m³/s) for the pressure and temperature of the liquid steel in the ladle. The factor λ is dimensionless.

Table 1. Physical Model with Water x Industrial Ladle: The Most Important Parameters.

	Industrial ladle (65 t)	Physical model (scale 1:3)
Liquid phase	Steel	Water
Liquid density (kg/m³)	7000	1000
Cinematic viscosity (m²/s)	0.91x10-6	1x10-6
Temperature (°C)	1600	25
Internal diameter (mm)	Max. 2282, Min. 2082	Max. 760, Min 694
Liquid height (mm)	2460	820
Liquid volume (m³)	9.4	0.340
H/D$_{Mean}$ relation	1.13	1.13
Gas injection device	Porous plug	Orifice, d=2 mm
Injected gas	Argon	Compressed air
Gas flow rate (Nl/min)	70	17

2.2 Dye tracer test

The technique of dye-tracer injection [4, 6] consists on adding a tracer substance, in this case a solution of potassium permanganate, to the liquid, observing its dispersion on both time and space. Supposing that the dye tracer do not interfere in the fluid flow dynamics, it is possible to visualize the fluid displacement for each one of the three different gas injection positions. Then, information about the state of the mixing in all regions of the ladle can be obtained while the time increases. The tests are registered by a CCD camera for posterior offline analysis.

The dye tracer test results have been obtained by Morales J.A. et al. [12], at a time of 12s after the fluid flow reached its stationary regime. These results are shown in Fig. 2a-c. In these tests, the tracer addition position A shown in Fig. 1 was used and a flow rate of 17 Nl/min was employed. These results will be compared qualitatively with the average velocity field presented in the section 3.

| (a) Gas Injection Position PT1 | (b) Gas Injection Position PT2 | (c) Gas Injection Position PT3 |
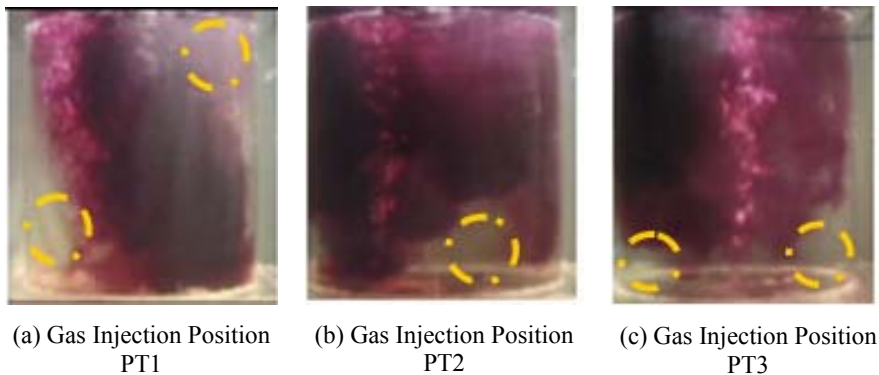
Fig. 2. Dye Tracer Test for Different Gas Injection Positions. Circles: Dead Zones.

2.3 Mixing time

With the experimental arrangement showed in Fig. 1, the mixing time was determined considering a criterion of a mixing degree of 95% [2, 3, 4, 9]. The mixing time at 95% was defined as the time necessary for the dye tracer concentration in the position where the sensor is to reach ±5% of its concentration in the stationary state. Five measurements of the mixing time were realized, taking the average value as the final result for the mixing time. The standard deviation of the individual values in this measurement was less than 16%.

The table 2 presents the experimental results for a mixing time of 95% for the three different gas injection positions, a tracer addition position A, and a gas flow rate of 17Nl/min. Refer to [12] for further details about these data. It can be observed that the average mixing time value are greater for the inferior sensor than the value of the superior sensor, serving as an indicator that the location chosen for the conductivity sensor is adequate [4, 6, 9].

Table 2. Mixing Time of 95% (in seconds) for the 3 Different Gas Injection Positions and a Gas Flow Rate of 17 Nl/min.

Sensor	Gas Injection Position PT1	Gas Injection Position PT2	Gas Injection Position PT3
Superior	58.7	52.7	57.2
Inferior	83	57	68.5

2.4 Velocity field determination

Fig. 3 shows the experimental equipments employed in the measurements. This instrumentation system is composed of an air compressor, a pressure regulator and a rotameter. The physical model was cross sectioned by two illumination planes, named here of LASER Sheet A and LASER Sheet B. These planes have been chosen as an attempt to extract three-dimensional information about the structure of the fluid flow. It was expected by us that the LASER Sheet B will provide additional information for the characterization of the fluid flow achieved with LASER Sheet A.
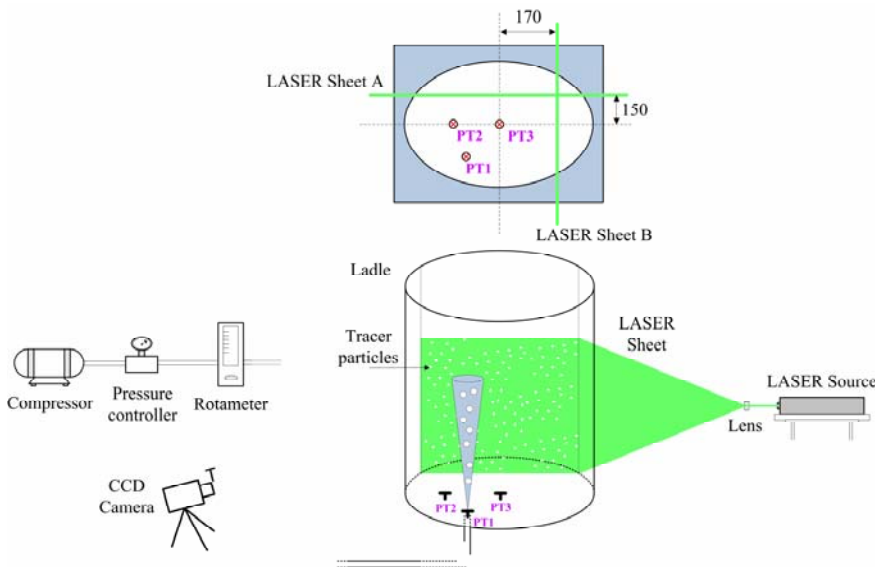
Fig. 3. The Physical Model of the Ladle and the Instrumentation System Employed in the Measurement of the Velocity Fields of the Fluid Flow.

In order to obtain the velocity field of the fluid flow, the Image Processing Velocimetry technique was employed [7]. With such a technique, small tracer particles are inserted in the fluid flow, which is irradiated by a LASER. The LASER light spread by the particles is captured by a CCD camera (Charged Coupled Device), which analogically stores both the space and time evolution of particles at a rate of 30 Q/s.

The captured recording is digitized by a frame grabber connected to a PC, where it is stored in AVI format. Later, it is divided into their constituent frames, which are stored in Bitmap (BMP) images. Each frame represents the spatial behaviour of the fluid flow in a particular time. The sequence of frames provides the information about the fluid flow dynamics.

The particle density employed in the tests determined the operation of the system in the PIV (Particle Image Velocimetry) mode [11]. Thus, statistical algorithms based on the cross-correlation between interest and search areas previously selected in the frames captured from the fluid flow were employed.

The frames captured from the fluid flow by the CCD camera are subdivided in interest areas. The size of the interest areas must be previously determined by the experimentalist and is directly related with the superficial particle density in the frame. As greater is the particle density, smaller interest areas can be selected.

For a greater density of vectors in the measured velocity fields, it was used an overlapping technique in the selection of the interest areas [7]. The two dimensional velocity vector of a given particle group internal to the interest area was obtained by the cross correlation of one interest area in an instant of time t and another in an instant of time t+Δt. Finally, the whole velocity field was obtained by the calculation of all vectors of all interest areas that compose the frames captured from the fluid flow under analysis. A detailed discussion about the software architecture of the computational tool developed by us and used here to measure the velocity fields can be found in reference [8].

For the LASER sheet formation, it was used an argon ion source type (model Innova 70, 5W), which was coupled into cylindrical lens by an optical fibber. This optical fibber carries the LASER beam from the source until the ladle. Also it gives mobility and flexibility to its application with different arrangements of equipments employed for the LASER sheet formation in other flow configurations.

Polyethylene particles were used as a tracer in these measurements. Polyethylene is a white polymer with well light reflection properties. The particles were obtained by the smash of small pieces of this polymer in a mill. The resulted particles were analyzed in the CILAS equipment. Its mean diameter was 150 meshes (100 μm).

3.   Results and discussion

Fig. 4-6 show the time-average velocity fields at a time of 12s for the different gas-injection positions previously described PT1, PT2, and PT3 and for a gas flow rate of 17Nl/min. In the Fig. 4-6a, it is shown the velocity fields measured through the LASER Sheet A while, in the Fig. 4-6b, it is shown the velocity fields measured with the LASER Sheet B. By a qualitative analysis of these time-average velocity fields, it is possible to identify the fluid flow structure generated by each one of the gas-injection positions. Also, it is possible to extract information to better understand the behaviour of the dye tracer observed in the tests shown in the section 2.2, identifying the low velocity regions of the ladle and its relation with the dead zones. All vectors presented in these figures are in scale and has been plotted over the first frame used in the time-average process.

For the eccentric gas injection position PT1, the velocity field from the frontal view of Fig. 4a presents a vortex on the left side, close to the ladle surface and to the ladle wall, as well as another vortex close to the central axis of the ladle and to the ladle bottom. The lateral view, which is presented in the Fig. 4b, complements this vortex characterization. However, according to the velocity fields presented in Fig. 4a, the regions belonging to both the right superior and the left inferior edge are weakly influenced by those vortexes. The result is a major amount of movement in the diagonal direction, connecting the left superior edge to the right inferior one. Furthermore, this is evidence that both the right superior and the left inferior regions will take longer to be mixed with the dye tracer.

Comparing the velocity field shown in Fig. 4a with the dye tracer results of Fig. 2a, for an eccentric gas injection position PT1, it can be observed that the dye tracer path is coherent with the high velocity regions in the right side of the lateral view of Fig. 4b. This means that the dye tracer cloud is dispersed from the surface in direction to the ladle bottom through a clockwise rotational movement of the fluid.

(a)   (b)
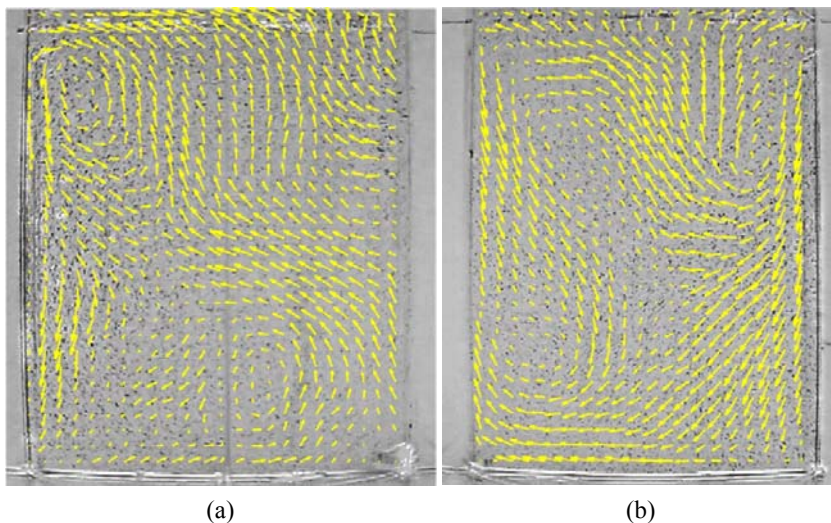
Fig. 4. Average Velocity Field at t=12s for the Eccentric Gas Injection Position PT1: (a) The Frontal View (LASER sheet A), and (b) The Lateral View (LASER sheet B). Gas Flow Rate of 17 Nl/min.

The characteristic of rotational fluid flow obtained with the gas-injection position PT1, qualitatively analysed through both the dye tracer and the image processing velocimetry tests showed here, have been also observed by Joo S. and Guthrie R.I.L. [2] for eccentric positions in relation to the central gas injection position. There is a belief that the high mixing times presented by the gas position PT1 are related to an excessive injector eccentricity, which favours the wall effect; that is, the contact of bubble plume with the model walls, as shown in Fig. 2a. Such a wall effect may reduce the transference of stirring energy to the bath, increasing mixing times for this eccentric position in relation to other gas injection positions. Joo S. and Guthrie R.I.L. [2] and Becker J. with Oeters F. [6]

also reported such behaviour in a model of the same scale used in the present study, but with a cylindrical shape.

For the half radius position PT2, whose frontal and lateral views are shown in Fig. 5, it can be observed a fluid flow with a great amount of small recirculation zones distributed throughout the bath, with higher velocities at the ladle bottom when it is compared with the central gas-injection position PT3, as it will be shown by us later when analyzing its velocity fields. Those small vortexes distributed inside the ladle are an important factor to improve and to turn the liquid mixing inside the ladle faster when compared with the other gas-injection positions.

For the stirring by the half radius position PT2, a comparison between the time-average velocity field of the frontal view, presented in Fig. 5a, with the dye tracer dispersion, presented in Fig. 2b, shows that the obtained results seems to be coherent. That is, the region where the dye tracer mixes at last approaches the region with low velocity in the center of the ladle bottom, according to the frontal view of Fig. 5a, and in the left inferior edge of the lateral ladle view of Fig. 5b. The mixing-time reduction presented by the half-radius gas position PT2 is consistent with results obtained by other researchers [2, 3, 4, 13, 14]. They observed that when the injector position moves on from the ladle center to its wall, mixing times decrease. Furthermore, they attributed the mixing time reduction to eddies formation [15], which is a characteristic observed in that situation.
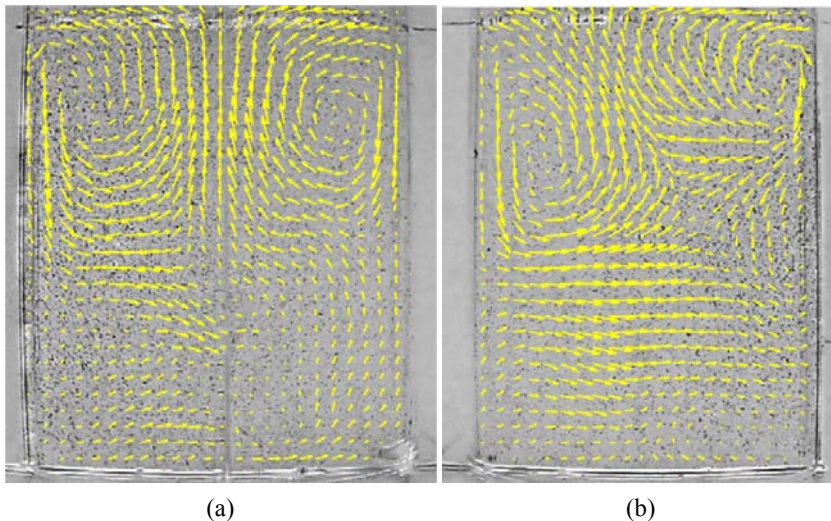

(a)   (b)
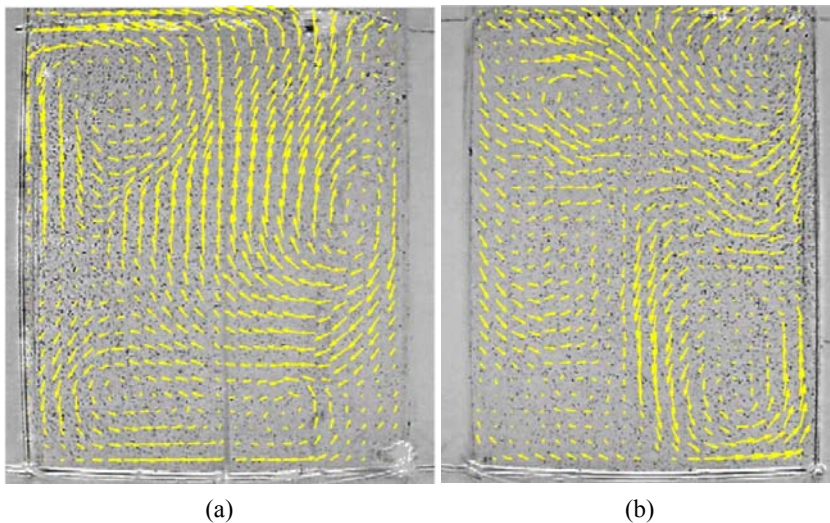
Fig. 5. Average Velocity Field at t=12s for the Half Radius Gas Injection Position PT2: (a) The Frontal View (LASER Sheet A), and (b) The Lateral View (LASER Sheet B). Gas Flow Rate of 17 Nl/min.

During the stirring for a central injection position PT3, it can be observed, in the frontal view shown in Fig. 6a, two symmetrical recirculation regions of the liquid close to the surface, and in both sides of the ladle wall. There are some

regions with low velocities at the ladle bottom, which are consistent with the behaviour observed in the dye tracer test from Fig. 2c. The two vortexes present opposite rotation directions, originating a high rising fluid flow in the central region that is strongly dispersed when the water-air interface is excited at the ladle surface.

In the lateral view of the ladle presented in Fig. 6b, the ascendant fluid behaviour shown in Fig. 6a is complemented. A transverse flow below of the half ladle body demonstrates the existence of a vortex with dimensions and parallel to the ladle base. This vortex makes the stirring of the fluid in the ladle bottom more difficult.

A comparison of the velocity field of the frontal view shown in the Fig. 6a with the dye tracer test shown in Fig. 2c, during the stirring for a central gas injection position PT3, determines that the regions in inferior edges of the ladle where the mixing performs at last corresponds to the low velocity regions of the flow. The increase of mixing times for the central gas injection position PT3 is related to the existence of dead zones in the ladle edge, as it is seen both in the dye tracer test in Fig. 2c, and qualitatively in the velocity field of Fig. 6. Those results are consistent with experimental results obtained by other researchers [2, 3, 4, 5] who carried out such experiments in physical models of cylindrical ladles.

(a)   (b)

Fig. 6. Average Velocity Field at t=12s for Central Gas Injection Position PT3: (a) The Frontal View (LASER Sheet A), and (b) The Lateral View (LASER Sheet B). Gas Flow Rate of 17 Nl/min.

The dye tracer tests results shown in the Fig. 2 induce to think that a more homogeneous mixing happens for a gas-injection with position PT2. The mixing times of table 2 also indicates that the fastest mixing happens in this gas-injection position. As the velocity field structure shown in Fig. 5a, this fact is possibly associated with the existence of a greater number of small vortexes distributed inside the ladle and with the existence of a lower number of low velocity regions in the generated fluid flow.

The mixing times of table 2 indicates that the second better mixing occurs for the gas injection position PT3. However, with just a qualitative analysis of the dye tracer tests and the measured velocity fields, it becomes difficult to assure if PT3 really offers a better mixing than PT1, or vice-versa. This circumstance demands that future researches include a quantitative analysis of the measured velocity fields.

4. Conclusions

In this work, it has been presented by us a qualitative analysis of the velocity fields measured through the PIV technique for three different gas injection positions in an acrylic physical model of an elliptical siderurgical ladle. This qualitative analysis of the velocity field propitiated to identify the different fluid flow structures that are developed inside the ladle for each one of the gas-injection positions employed in the tests. This information shows to be important to relate which characteristics of the fluid flow structure influences over the mixing phenomenon. This is a starting point for future quantitative analysis.

The analysis of the velocity fields shows 3 so different fluid flow structures for each one of the employed gas injection positions. As a summary, the fluid flow obtained with the gas injection position PT1 has been mainly characterized by two high intensity vortexes, one in the frontal view, at the superior left corner of the ladle, and one in the lateral view, at the superior right corner of the ladle. For the gas injection position PT2, it is observed a large quantity of considerable small vortexes disseminated over the both lateral and frontal view of the ladle. For the last one, the fluid flow structure generated by the gas injection through PT3 is characterized by 2 high intensity vortexes at the superior half of the ladle body. These vortexes continuously excites this ladle region, ejecting fluid upward and originating dissipation of its energy when it reaches the water-air interface at the ladle surface. The inferior half of the ladle body remains almost unchanged for this gas injection position.

The analysis of the velocity fields indicated that the distribution of small size and numerous vortexes in the fluid flow is a key factor for obtaining better mixings inside the ladle. Possibly, a more homogeneous mixing is related with the number and the size of the vortexes that were created and persists in the fluid flow by a time. A large number of small vortexes possibly determine that an improvement in the mixing quality will be achieved. Also, a more fast mixing will happen in the situations where the fluid flow structure has fewer regions with low velocity. In this way, due to the characteristics above, a better mixing should be obtained with the gas injection position PT2. However, this is just an indicative. Quantitative analysis of the measured velocity fields have to be carried out to confirm this assumption.

5. Future works

In future works, quantitative results will be extracted from the velocity fields presented here. Therefore, local parameters as vorticity, intensity of turbulence, and Reynolds stress will be computed and compared for each one of the gas injection positions. In this way, it will be expected by us to exactly determine which are the influences of PT1, PT2, and PT3 gas-injection positions in the generated fluid flow and, as a consequence, its exactly influences over the mixing phenomenon.

Acknowledgements

References

1. Mazumdar, D. & Guthrie, R.I.L. (1995). The Physical and Mathematical Modeling of Gas Stirred Ladle Systems. *ISIJ International*.35(1), 1-20.

2. Joo, S. & Guthrie, R.I.L. (1992). Modeling Flow and Mixing in Steelmaking Ladles Designed for Single- and Dual-Plug Bubbling Operations. *Metallurgical Transactions B*. 23B, 765-778.

3. Zhu, M.Y., Inomoto, T., Sawada, I. & Hsiao, T.C. (1995). Fluid flow and mixing phenomena in the ladle stirred by argon through multi-tuyere. *ISIJ International*, Vol. 35, No. 5, p. 472-479.

4. Mietz, J. & Oeters, F. (1988). Model Experiments on Mixing Phenomena in Gas-Stirred Melts. *Steel Research*. 59(2), 52-59.

5. Mietz, J. & Oeters, F. (1989). Flow field and mixing with eccentric gas stirring. *Steel Research 60*, No. 9, p. 387-394.

6. Becker, J. & Oeters, F. (1998). Model Experiments of Mixing in Steel Ladles with Continuous Addition of the Substance to be Mixed. *Steel Research*. 69(1), 8-16.

7. Nunes R.P. (2005). Projeto e Implementação de um Sistema de Instrumentação Eletro-Eletrônica Para Caracterização de Escoamentos através de Processamento Digital de Imagens. Master of Science Dissertation. UFRGS, Porto Alegre, RS, Brazil.

8. Nunes R.P. & van der Laan, F.T. (2007). Design of A Software Architecture for Velocimetry Systems. *Journal of Computer Science*. 6 (3). In Press.

9. Mazumdar, D., Kim, H.B. & Guthrie, R.I.L. (2000). Modeling Criteria for Flow Simulation in Gas Stirred Ladles: Experimental Study. *Ironmaking Steelmaking*. 27(4), 302-309.

10. Mazumdar, D. (2000). Some Fundamental Considerations Concerning Gas Injection Operations in Steelmaking Ladles. In *Proc. Ironmaking Conference* 59, Softbound, Pittsburgh, Pennsylvania, 531-540.

11. Adrian, R.J. (1991). Particle-Imaging Techniques for Experimental Fluid Mechanics. *Annual Review of Fluid Mechanics*. 23, 261-304.

12. Morales, J.A, François, M.G., Ribeiro, J.L.D. & Vilela, A.C.F. (2006). Variation on the Geometric Profile of A Steel Ladle and its Effect on the Mixing. *Steel Grips*. 4(1), 34-39.

13. Akdogan, G. & Eric, R.H. (1999). Model Study on Mixing and Mass Transfer Ferroalloy Refining Processes. *Metallurgical and Materials Transactions*. 30B, 231-239.

14. Asai, S., Okamoto, T., He, J.C. & Muchi, I. (1983). Mixing Time of Refining Vessels Stirred by Gas Injection. *Transactions ISIJ*. 23, 43-50.

15. Szekely, J. (1979). *Fluid Flow Phenomena in Metals Processing*. USA: Academic Press- Inc.